Modeling and Simulation of NO_x Absorption in Pilot-Scale Packed Columns

N. J. Suchak, K. R. Jethani, and J. B. Joshi
Dept. of Chemical Technology, University of Bombay, Matunga, Bombay, 400 019, India

Absorption of nitrogen oxides was studied in three packed columns in series. Two were 254 mm ID and 6 m tall, the third was 800 mm ID and 3 m tall. Absorption was also studied in two packed columns of 800 mm ID, 7 and 10 m tall, operated in series. Solutions of mixed nitric and sulfuric acids were used as absorbents. Specific rates of absorption were measured using a stirred cell with a flat interface.

A mathematical model is developed for an adiabatic operation. The gas phase reactions and equilibria, gas phase mass transfer, interface equilibria, and liquid phase reactions are included in the model. Heterogeneous gas–liquid equilibria are included in the model for the first time. The variation in the rates of absorption with chemical reaction (of NO_2, N_2O_3, and N_2O_4) with respect to acid concentration is considered. The formation of nitric acid in the gas phase is also considered in the model. Favorable agreement is shown between the model predictions and the experimental observations.

Introduction

Absorption of NO_x gas is an important step in the manufacture of nitric acid. The removal of NO_x from the off-gases/flue gases has received considerable attention due to stringent statutory regulations for a clean environment.

Absorption of NO_x gas is probably the most complex when compared with other absorption operations. The reasons are:

1. The NO_x gas is a mixture of several components consisting of N_2O, NO, NO_2, N_2O_3, N_2O_4, N_2O_5, etc., and the absorption of NO_x gas in water results into two oxyacids, nitric acid and nitrous acid.

2. Several reversible and irreversible reactions occur in both gas and liquid phases.

3. Simultaneous absorption of many gases occurs followed by chemical reaction. Also, simultaneous desorption of many gases occurs preceded by chemical reaction. For example, the absorption of NO_2, N_2O_3, and N_2O_4 is accompanied by chemical reaction whereas the desorption of NO, NO_2, and HNO_2 is preceded by chemical reaction.

4. Heterogeneous equilibria prevail between gas phase and liquid phase components.

Sherwood et al. (1975) and Joshi et al. (1985) have reviewed these aspects of NO_x absorption.

Correspondence concerning this article should be addressed to J. B. Joshi.

For the process design of NO_x absorption towers, it is necessary to understand the combined effects of several equilibria, the rates of mass transfer, and chemical reaction. Further, substantial heat effects are associated with NO_x absorption; therefore, temperature variations need to be taken into account in the process design. There have been outstanding attempts in this direction. For instance, Koval and Peters (1960), Andrew and Hanson (1961), Koukolik and Marek (1968), Carleton and Valentin (1968), Hoftizer and Kwanten (1972), Makhotkin and Shamsutdinov (1976), Holma and Sohlo (1979), Emig et al. (1979), Counce and Perona (1979a,b, 1980, 1983), Joshi et al. (1985), and Selby and Counce (1988) have reported various aspects of the process design of packed columns, plate columns, and packed bubble columns used for the manufacture of nitric acid. These attempts will be strengthened if the following important features are included in the process design.

1. The rates of absorption of NO_2, N_2O_3, and N_2O_4 in nitric acid are different from those in water. The rates decrease with an increase in the concentration of nitric acid.

2. It is known that, for a given set of partial pressures of NO, NO_2, and N_2O_4, there exists a certain limiting concentration of nitric acid beyond which no absorption of N_2O_4 and NO_2 occurs (Carberry, 1958). This heterogeneous equilibrium substantially reduces (even three to four times) the rates of

absorption of NO_2, N_2O_3, and N_2O_4, and the extent of reduction increases as the nitric acid concentration approaches the equilibrium value. This aspect has not been included in the mathematical models reported so far.

3. A substantial quantity of nitric acid is formed in the gas phase, particularly at high temperatures and high partial pressures of NO_x. Therefore, HNO_3 formation needs to be included in the mathematical model.

4. A detailed energy balance also needs to be incorporated in the model.

The mathematical model presented in this work includes the above four features.

Simulation of large-size absorbers increases confidence in the model development. In the published literature, although some experimental data have been collected on pilot-scale absorbers, the absorbent was invariably water except in the investigation carried out by Counce and Perona (1983). There is scant information available regarding large-scale simulation. Further, there has been no study when the nitric acid contains some other electrolyte. Therefore, it was thought desirable to simulate large-scale absorbers. Solutions of mixed nitric and sulfuric acids were used as solvents. A comparison is presented between the model predictions and the experimental observations.

Mathematical Model

Model for overall rate of absorption

Gas Phase Reactions and Equilibria. NO_x is a mixture of various nitrogen oxides, NO, NO_2, N_2O_3, and N_2O_4. In the presence of water vapor, which is generally the case in most industrial absorbers, there exist the oxyacids HNO_2 and HNO_3. All the components of NO_x are in equlibrium with each other. Nitric oxide undergoes irreversible oxidation with oxygen in the gas phase. The oxidation reaction is expressed as:

$$2NO_{(g)} + O_{2(g)} \xrightarrow{k_1} 2NO_{2(g)} \tag{1}$$

Joshi et al. (1985) have reviewed the published literature on NO oxidation. It is believed that NO oxidation proceeds by dimerization of NO followed by oxidation by oxygen to form N_2O_4. The oxidation reaction is second order with respect to NO and first order with respect to oxygen. However, below 250 ppm of NO_x, the reaction is first order in both NO as well as O_2.

Complex equilibria prevail in the gas phase, which can be described by following equations:

$$2NO_{2(g)} \overset{K_2}{\rightleftharpoons} N_2O_{4(g)} \tag{2}$$

$$NO_{(g)} + NO_{2(g)} \overset{K_3}{\rightleftharpoons} N_2O_{3(g)} \tag{3}$$

$$NO_{(g)} + NO_{2(g)} + H_2O_{(g)} \overset{K_4}{\rightleftharpoons} HNO_{2(g)} \tag{4}$$

$$3NO_{2(g)} + H_2O_{(g)} \overset{K_5}{\rightleftharpoons} 2HNO_{3(g)} + NO_{(g)} \tag{5}$$

The reaction rate constant k_1 and the gas phase equilibria constants K_2 . . . K_5 were reported by Joshi et al (1985) and are summarized in Table 1.

Table 1. Gas Phase Reactions

Eq. No.	Equilibrium and Rate Constants
1	$\log_{10} K_1 = 652.1/T - 0.7356$ atm$^{-1}\cdot$s^{-1}
2	$\log_{10} K_2 = 2{,}993/T - 9.226$ atm^{-1}
3	$\log_{10} K_3 = 2{,}072/T - 7.234$ atm^{-1}
4	$\log_{10} K_4 = 2{,}051.17/T - 6.7328$ atm^{-1}
5	$\log_{10} K_5 = 2{,}003.8/T - 8.757$ atm^{-1}

Rates of Gas Phase Mass Transfer. The concentration profiles for the gas film are shown in Figure 1. The volumetric rates of gas phase mass transfer are given by the following equations:

$$Ra_{NO,G} = (k_G\underline{a})_{NO}\,[p^i_{NO} - p^o_{NO}] \tag{6}$$

$$Ra_{NO_2,G} = (k_G\underline{a})_{NO_2}\,[p^o_{NO_2} - p^i_{NO_2}] \tag{7}$$

$$Ra_{N_2O_4,G} = (k_G\underline{a})_{N_2O_4}\,[p^o_{N_2O_4} - p^i_{N_2O_4}] \tag{8}$$

$$Ra_{N_2O_3,G} = (k_G\underline{a})_{N_2O_3}\,[p^o_{N_2O_3} - p^i_{N_2O_3}] \tag{9}$$

$$Ra_{HNO_3,G} = (k_G\underline{a})_{HNO_3}\,[p^o_{HNO_3} - p^i_{HNO_3}] \tag{10}$$

$$Ra_{HNO_2,G} = (k_G\underline{a})_{HNO_2}\,[p^o_{HNO_2} - p^i_{HNO_2}] \tag{11}$$

$$Ra_{H_2O,G} = (k_G\underline{a})_{H_2O}\,[p^i_{H_2O} - p^o_{H_2O}] \tag{12}$$

At this stage, the following points may be noted.

1. In the gas film, the partial pressure of NO changes with respect to distance from the interface up to the bulk gas. It is likely that the rate of NO oxidation in the film is different from the rate in the bulk. Further, the transfer of NO is accompanied by oxidation. Therefore, there is a possibility of enhancement in the rate of mass transfer.

The volume of the gas film can be estimated on the basis of D_G, k_G, H, and $\underline{a}$. It was found that the film volume constitutes about 0.005-0.01 of the total volume. Therefore, the extent of NO oxidation in the film was negligible and there was no appreciable enhancement in the mass transfer rate of NO due to chemical reaction.

2. In the gas film NO, NO_2, N_2O_3, N_2O_4, HNO_2, HNO_3, and water were assumed to be in equilibrium at all points. The rates of gas phase mass transfer are likely to change due to the equilibrium reactions. However, for simplicity, the gas phase mass transfer rates have been written in the form of Eqs. 6 to 12. Similar assumptions have been made by Andrew and Hanson (1961), Carleton and Valentine (1968), Emig et al. (1979), and Holma et al. (1979).

Interface Equilibria. At the interface, NO, NO_2, N_2O_3, N_2O_4, and HNO_2 are assumed to be always in equilibrium with each other. Thus, at the interface, gas equilibria are defined by following equations:

$$K_2 = \frac{p^i_{N_2O_4}}{(p^i_{NO_2})^2} \tag{13}$$

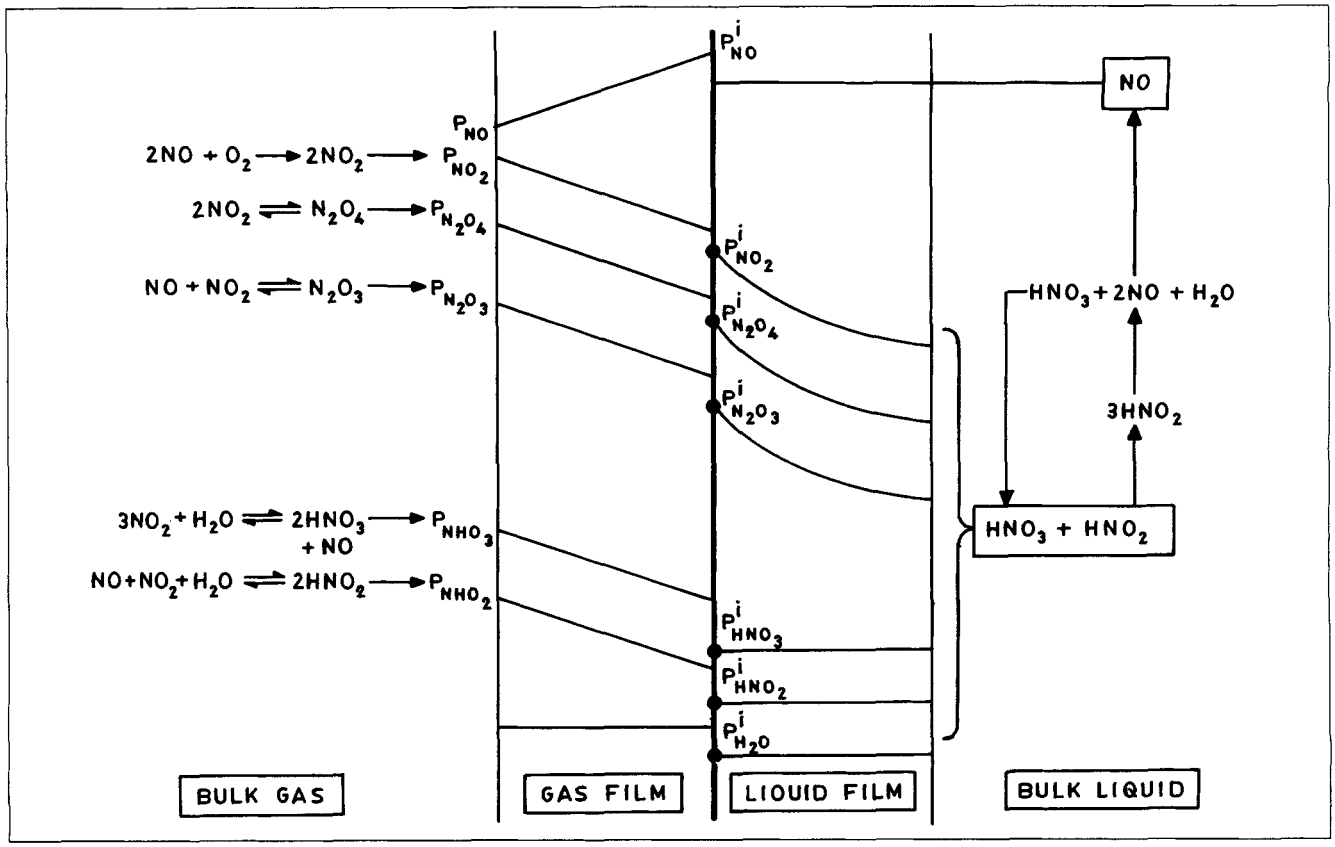

Figure 1. Mechanism of NO_x absorption into water.

$$K_3 = \frac{p^i_{N_2O_3}}{(p^i_{NO})\ (p^i_{NO_2})} \tag{14}$$

$$K_4 = \frac{(p^i_{HNO_2})^2}{(p^i_{NO})\ (p^i_{NO_2})\ (p^i_{H_2O})} \tag{15}$$

HNO_3 and H_2O are at their saturation concentrations at the interface. The vapor pressure of H_2O or HNO_3 over aqueous sulfuric acid solution is a function of temperature and nitric acid concentration:

$$p^i_{H_2O} = f\,[T,\ \text{conc}\,(HNO_3)] \tag{16}$$

$$p^i_{HNO_3} = f\,[T,\ \text{conc}\,(HNO_3)] \tag{17}$$

$$p^i_x\, H_x = [A^*]_x \tag{18}$$

where x denotes the component. The values of H_x have been compiled by Joshi et al. (1985).

Liquid Phase Reactions. Nitrogen oxides when absorbed in aqueous sulfuric acid solution, form nitrous and nitric acid. The following reactions occur in the liquid phase:

$$2NO_{2(l)} + H_2O_{(l)} \rightarrow HNO_{3(l)} + HNO_{2(l)} \tag{19}$$

$$N_2O_{3(l)} + H_2O_{(l)} \rightarrow 2HNO_{2(l)} \tag{20}$$

$$N_2O_{4(l)} + H_2O_{(l)} \rightarrow HNO_{2(l)} + HNO_{3(l)} \tag{21}$$

HNO_2 in bulk in the liquid phase is considered to be decomposing to form nitric acid:

$$3HNO_{2(l)} \rightarrow HNO_{3(l)} + 2NO_{(l)} + H_2O_{(l)} \tag{22}$$

Mass Transfer with Chemical Reaction in the Liquid Film. The concentration profiles for different species in the liquid film are given in Figure 1. It has been illustrated by Joshi et al. (1985) that the absorption of NO_2, N_2O_3, and N_2O_4 is accompanied by chemical reaction within the liquid film. However, absorption of NO_x is also limited by nitric acid concentration in the liquid phase bulk and the partial pressure of NO at the interface. Carberry (1958) made a plot of maximum attainable concentration of nitric acid as a function of parameter K_6 defined as

$$K_6 = \frac{p^i_{NO}}{(p^b_{N_2O_4})^{3/2}} \tag{23}$$

An empirical equation (Matasa and Tonca, 1973) obtained from various plots is of the form:

$$\ln K_H = 2.188 \times 10^7\ T^{-2.58} - 4.571 \times 10^4\ T^{-1.424} W \tag{24}$$

where

$$K_H = \frac{p_{NO}}{p_{NO_2}^3} = K_2^{3/2} K_6 (101.33)^2 \quad (25)$$

and W is the maximum attainable HNO_3 concentration in weight fraction. The method for determining K_6 in the presence of sulfuric acid is discussed later.

The limiting partial pressures of NO_2, N_2O_3, and HNO_2 based on heterogeneous equilibria would be

$$p^b_{NO_2} = \left(\frac{p^b_{N_2O_4}}{K_2}\right)^{1/2} \quad (26)$$

$$p^b_{N_2O_3} = K_3\, p^b_{NO}\, p^b_{NO_2} \quad (27)$$

$$p^b_{HNO_2} = (K_4\, p^b_{NO}\, p^b_{NO_2}\, p^b_{H_2O})^{1/2} \quad (28)$$

No absorption takes place when $p^i_{N_2O_4} = p^b_{N_2O_4}$. The net driving force is thus the difference between the interfacial and limiting partial pressures of NO_2, N_2O_4, N_2O_3, and HNO_2.

The volumetric absorption rates of different species are:

$$Ra_{NO_2,L} = \underline{a}\ (H_{NO_2})^{3/2}\ [2/3\ (kD)_{NO_2}]^{1/2}\ (p^i_{NO_2} - p^b_{NO_2})^{3/2} \quad (29)$$

$$Ra_{N_2O_4,L} = \underline{a}\ H_{N_2O_4}\ [(kD)_{N_2O_4}]^{1/2}\ (p^i_{N_2O_4} - p^b_{N_2O_4}) \quad (30)$$

$$Ra_{N_2O_3,L} = \underline{a}\ H_{N_2O_3}\ [(kD)_{N_2O_3}]^{1/2}\ (p^i_{N_2O_3} - p^b_{N_2O_3}) \quad (31)$$

$$Ra_{HNO_2,L} = k_L \underline{a}\ H_{HNO_2}\ (p^i_{HNO_2} - p^b_{HNO_2}) \quad (32)$$

Nitrous acid in bulk decomposes to form HNO_3 and NO in the liquid phase. Since the latter has limited solubility, it desorbs. The rate of desorption of NO is given as

$$Ra_{NO,L} = \frac{4}{3} Ra_{N_2O_3,L} + \frac{2}{3} Ra_{N_2O_4,L} + \frac{1}{3} Ra_{NO_2,L} + \frac{2}{3} Ra_{HNO_2,L} \quad (33)$$

Overall Volumetric Rates of Absorption. Overall rates of absorption are computed by solving Eqs. 6-18 and 23-33. There are twenty-three equations, whereas the unknowns are:

1. Volumetric rates of gas phase mass transfer: $Ra_{NO,G}$, $Ra_{NO_2,G}$, $Ra_{N_2O_4,G}$, $Ra_{N_2O,G}$, $Ra_{HNO_2,G}$, $Ra_{HNO_3,G}$, $Ra_{H_2O,G}$
2. Partial pressures of NO, NO_2, N_2O_4, N_2O_3, HNO_2, H_2O, and HNO_3 at interface: p^i_{NO}, $p^i_{NO_2}$, $p^i_{N_2O_4}$, $p^i_{N_2O_3}$, $p^i_{HNO_2}$, $p^i_{H_2O}$, $p^i_{HNO_3}$
3. Heterogeneous equilibrium parameter K_6, limiting partial pressures $p^b_{N_2O_4}$, $p^b_{NO_2}$, $p^b_{N_2O_3}$, $p^b_{HNO_2}$
4. Rates of mass transfer with chemical reaction in the liquid film: $Ra_{NO_2,L}$, $Ra_{N_2O_3,L}$, $Ra_{N_2O_4,L}$, $Ra_{HNO_2,L}$
5. Rate of desorption of NO from liquid to gas phase $Ra_{NO,L}$

Two more equations are needed to make the model consistent. These are provided by the material balance of divalent and tetravalent nitrogen oxides across the interface.

The NO_2 balance at the interface gives:

$$(Ra_{NO_2,G} - Ra_{NO_2,L}) = 2(Ra_{N_2O_4,L} - Ra_{N_2O_4,G}) + (Ra_{N_2O_3,L} - Ra_{N_2O_3,G}) + 1/2\ (Ra_{HNO_2,L} - Ra_{HNO_2,G}) \quad (34)$$

The NO balance at the interface gives:

$$Ra_{NO,L} - Ra_{NO,G} = (Ra_{N_2O_3,L} - Ra_{N_2O_3,G}) + 1/2(Ra_{HNO_2,L} - Ra_{HNO_2,G}) \quad (35)$$

Equations 16-18, 24, and 25 were solved independently while Eqs. 6-15, 23, and 26-35 are coupled algebraic equations. In order to attain convergence under varied parametric conditions, it was found necessary to reduce them to a set of two equations in terms of p^i_{NO} and $p^i_{NO_2}$. The procedure is described in appendix B.

Model for column performance

Model Equations. The packed column has been modeled for simulation studies. The following assumptions were made:

1. Gas and liquid phases flow in a countercurrent plug flow manner
2. Liquid holdup is uniform throughout the column
3. Gases follow ideal gas behavior
4. The column operates at steady state

Mass Balance. Mass balance across a differential height dh at height h from the bottom, Figure 2, results in the following differential equations.

Component balance in gas phase

a. Divalent nitrogen balance

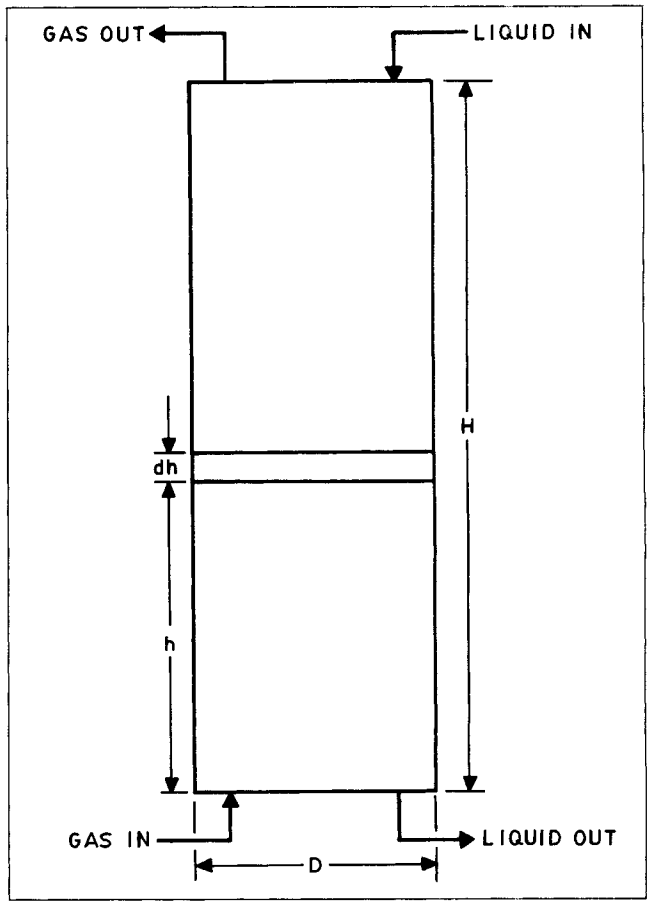

Figure 2. Differential element for mass and energy balances.

$$\frac{dY_{NO}^*}{dh} = -\frac{S}{G}\left[K_1 (P_{NO}^o)^2 P_{O_2}^o \epsilon_G - Ra_{NO,G} + Ra_{N_2O_3,G} + 0.5\,(Ra_{HNO_2,G} - Ra_{HNO_3,G})\right] \quad (36)$$

b. Balance for total reactive nitrogen

$$\frac{dY_N^*}{dh} = -\frac{S}{G}\left[-Ra_{NO,G} + Ra_{NO_2,G} + 2Ra_{N_2O_3,G} + 2Ra_{N_2O_4,G} + Ra_{HNO_3,G} + Ra_{HNO_2,G}\right] \quad (37)$$

c. Water-vapor balance

$$\frac{dY_{H_2O}^*}{dh} = -\frac{S}{G}\left[Ra_{H_2O,G} + 1/2Ra_{HNO_3,G} + 1/2Ra_{HNO_2,G}\right] \quad (38)$$

d. Oxygen balance

$$\frac{dY_{O_2}}{dh} = -\frac{1}{2}\frac{S}{G}\left[k_1 (p_{NO}^o)^2 (p_{O_2}^o) \epsilon_G\right] \quad (39)$$

Component balance in liquid phase

e. Balance for nitric acid

$$\frac{dX_{HNO_3}}{dh} = -\frac{S}{L}\left[4/3Ra_{N_2O_4,L} + 2/3Ra_{N_2O_3,L} + Ra_{HNO_3,G} + 2/3Ra_{NO_2,L} + 1/3Ra_{HNO_2,L}\right] \quad (40)$$

Equations 36–40 are coupled linear differential equations. Total mass balance is established across the differential height on solving these equations simultaneously.

Estimation of Design Parameters. Mahajani and Joshi (1990) have developed general design procedures and derived rational correlations for hydrodynamics and mass transfer characteristics in packed columns. The design parameters include gas- and liquid-side mass transfer coefficients and effective interfacial area. In addition, we need to know the values of diffusivity and solubility. Details are given in appendix C.

Specific rates of absorption of N_2O_4 were measured experimentally to estimate $H(kD)^{1/2}$ values. This is discussed in a later section.

Heat Balance. Oxidation of NO, formation of N_2O_3 and N_2O_4 in the gas phase, absorption of NO_2, N_2O_3, N_2O_4, and the liquid phase reactions are exothermic. The decomposition of HNO_2, however, is endothermic. Because of these reactions, significant heat changes occur. The values of physicochemical parameters such as reaction rate constants, equilibrium constants, solubilities, vapor pressures, and diffusivities depend upon temperature. Heat, liberated because of various reactions in the gas and liquid phases, has been included in Table 2. It will be assumed that the heat liberated is taken up by the liquid phase and the interface is always saturated with water vapor. Further, it was assumed that at any point in the column, the gas and liquid phase temperatures are the same.

If Q_T is the total heat change per unit time in the differential element, then the temperature change under adiabatic conditions is given by:

Table 2. Heats of Reaction

Reactions	Std. Heat of Reaction (25°C) kJ × 10^{-7}
Reactions in Gas Phase	
$2NO_{(g)} + O_{2(g)} \rightarrow 2NO_{2(g)}$	$\Delta H_1 = -5.7$ per kmol NO oxidized
$2NO_{2(g)} \rightarrow N_2O_{4(g)}$	$\Delta H_3 = -5.72$ per kmol N_2O_4 formed
$NO_{(g)} + NO_{2(g)} \rightarrow N_2O_{3(g)}$	$\Delta H_4 = -3.99$ per kmol N_2O_3 formed
$3NO_{2(g)} + H_2O_{(g)} \rightarrow 2HNO_{3(g)} + NO_{(g)}$	$\Delta H_6 = -1.77$ per kmol HNO_3 formed
$NO_{(g)} + NO_{2(g)} + H_2O_{(g)} \rightarrow 2\ HNO_{2(g)}$	$\Delta H_7 = -2.05$ per kmol HNO_2 formed
Reactions in the Liquid Phase	
Eq. D20 per kmol NO_2 absorbed	$\Delta H_8 = -5.36$
Eq. D21 per kmol N_2O_4 absorbed	$\Delta H_9 = -5.03$
Eq. D22 per kmol N_2O_3 absorbed	$\Delta H_{10} = -3.99$
Eq. D23 per kmol HNO_2 decomposed	$\Delta H_{13} = +2.39$
Eq. D24 per kmol HNO_3 absorbed	$\Delta H_{11} = -3.92$
Eq. D25 per kmol of HNO_2 absorbed	$\Delta H_{12} = -4.14$

$$T = \frac{Q_T}{m^o C_p^o} \quad (41)$$

where T is the temperature change across the differential element. Further details pertaining to the heat balance are given in appendix D.

Method of Solution

The method of solution involved the following five steps.

1. Estimation of gas phase composition

Equations A9–A11, appendix A, form a set of four simultaneous algebraic equations. The four unknowns are the mol/mol inerts of NO, NO_2, H_2O, and total moles in the gas phase. Equations were solved numerically by the Newton-Raphson matrix method for nonlinear equations.

2. Estimation of interface composition

For the estimation of interface composition, we need to solve twenty-one equations simultaneously, Eqs. 6–18, 23, and 26–32. The intricate algebraic reductions of these twenty-one equations into two polynomial equations, Eqs. A1 and A2, has obviated the need for a scaling algorithm. The variables selected—the interfacial partial pressures of NO and NO_2—are always present in greater magnitude than other components of NO_x. These two equations were numerically solved by the Newton-Raphson and Gauss-Jordan method. The main objective behind using this composite technique, which was algebraic and analytical in nature, was to achieve a single positive finite solution with minimum numerical iterations. Substituting these values in Eqs. 13–15, 23, and 26–28 results in the interfacial and limiting partial pressure values of N_2O_4, N_2O_3, and HNO_2.

3. Estimation of $H_x(kD)_x^{1/2}$ values

Absorption of NO_2, N_2O_3, and N_2O_4 in water has been extensively studied in the literature. Joshi et al. (1985) have critically reviewed the previous work. Kameoka and Pigford (1977) have shown that the rates of absorption of N_2O_4 in water and aqueous sulfuric acid solution are practically the same. They carried out experiments with 0.09 NH_2SO_4 solutions. At higher concentrations of sulfuric acid, the rates are likely to decrease. Further, in the present work the absorbent is a mixture of sulfuric and nitric acids at different concentrations. The kinetics of absorption of NO_x in mixed acid solutions has not been studied in the past. Therefore, it was thought desirable to undertake a systematic investigation. The details are given later.

4. Solutions of ordinary differential equations

Equations 36-40 are five coupled ordinary differential equations. Further, they constitute a boundary value problem. The flow rate and composition of the incoming gas phase are known. Similarly, the flow rate and concentration of incoming mixed acid (at the top of the column) are known. The equations were solved simultaneously by the fourth-order Runge-Kutta method. To start the integration procedure, the concentration of outgoing nitric acid (at the bottom of the column) was assumed. Integration was carried out up to the top of the column. A comparison was made between the calculated and the actual concentration of nitric acid. For convergence, the guess value at the bottom of the column was varied using the method of interval halving.

5. Solution of heat balance equations

From steps 1-4 the concentrations of all the species are known at the inlet and exit of a differential height. The rates of chemical reaction and mass transfer are also known. Assuming that all the sensible heat is taken up by the liquid phase, the change in temperature across the differential height was estimated. For this purpose Eqs. D1-D27, appendix D, were used.

Discussion of the Model

In the mathematical model developed in this work, four new features have been included:

1. The reduction in the rates of absorption of NO_2, N_2O_3, and N_2O_4 with respect to HNO_3 concentration was included by selecting appropriate values of $H(kD)^{1/2}$ in Eqs. 29, 30, and 31. The values of $H(kD)^{1/2}$ for the case of absorption in water have been summarized by Joshi et al. (1985). The variation of $[H(kD)^{1/2}]_{N_2O_4}$ with respect to HNO_3 concentration has been reported by Lefers and Van der Berg (1982). The same variation was assumed in the case of NO_2 and N_2O_3 absorption.

2. The heterogeneous equilibria between gas and liquid phase species have been included through Eqs. 23-28.

3. Complete heat balance has been established.

4. Provision was made for the formation of HNO_3 in the gas phase, Eq. 5.

Some results will now be given to demonstrate the relative importance of these features.

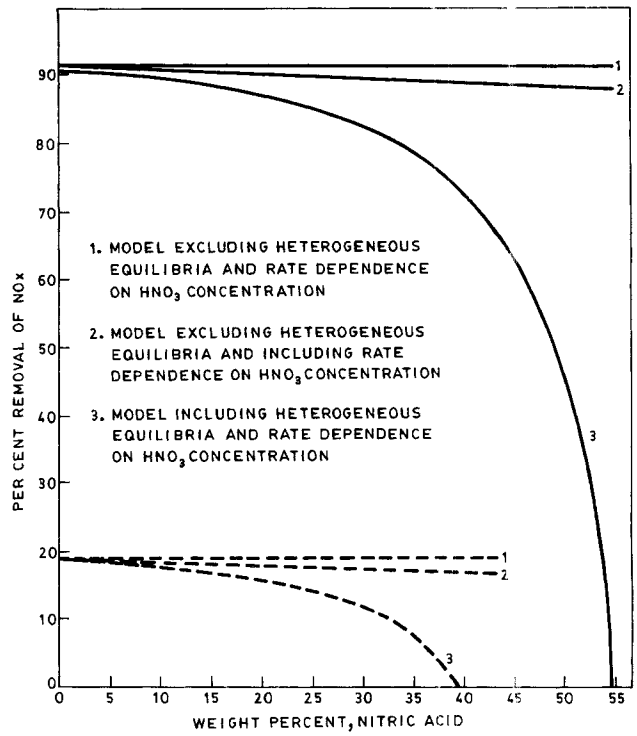

Figure 3. Effect of nitric acid concentration on extent of NO_x absorption.

NO_x flow rate = 0.99×10^{-4} kmol/s
Inerts flow rate = 2.15×10^{-4} kmol/s
Liquid inlet temperature = 303 K
Liquid superficial velocity = 7 mm/s
——Air flow rate = 5.1×10^{-4} kmol/s
----- Air flow rate = 0.0 kmol/s

Figure 3 shows the relative importance of the rate dependences on the NHO_3 concentration and the heterogeneous equilibria. In one set of experiments (solid lines) air was added to NO_x gas, whereas in the second set (broken lines) air was not added. In both of the sets the rate dependence on HNO_3 concentration has a small effect on the extent of NO_x removal. However, the heterogeneous equilibria markedly influence the rates of absorption. First of all, the heterogeneous equilibria successfully predict the maximum attainable concentration of HNO_3 for a given gas phase NO_x composition and temperature (for instance, 54% in set 1 and 39% in set 2). If this feature is not included, then it can be seen from Figure 3 that the extent of NO_x removal does not depend appreciably on HNO_3 concentration.

The role of heterogeneous equilibria with respect to NO_x composition is shown in Figure 4. It can be seen that the extent of NO_x removal strongly depends upon HNO_3 concentration.

The effect of energy balance is shown in Figure 5. It can be seen that the rise in temperature, as expected, reduces the extent of absorption. Therefore, the extent of NO_x removal in the isothermal case is higher than in the adiabatic case. It is obvious that the difference in these two cases will depend upon the temperature difference across the column.

The formation of HNO_3 in the gas phase was found to be substantial when NO_2^* partial pressure and temperature are high. It was found that the gas phase HNO_3 formation can

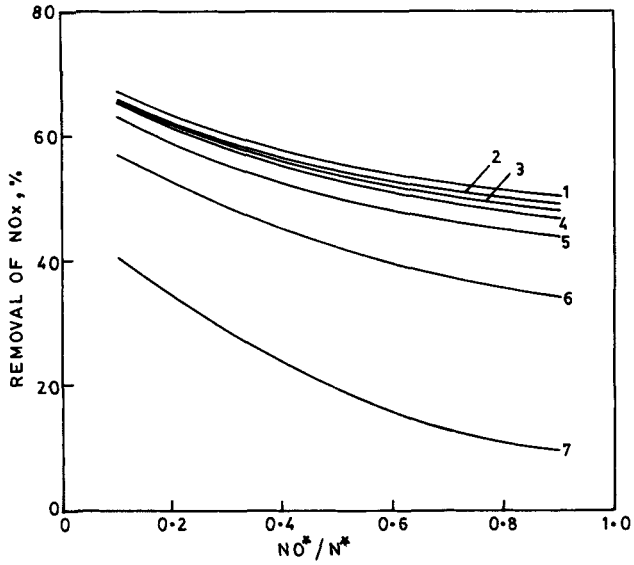

Figure 4. Effect of nitric acid concentration on extent of NO_x absorption.

Packed column dia. = 0.6 m, ht. = 1.0 m
Packing = 38 mm Intalox saddles
Liquid superficial veloc. = 6 mm/s
Gas superficial veloc. = 0.1 m/s
$k_G a = 1.25 \times 10^{-3}$ kmol/m^3·s·(kN/m^2)
$k_L a = 1.5 \times 10^{-2} \cdot s^{-1}$
$a = 125$ m^2/m^3
Liquid inlet temp. = 298 K
Total press. = 101.33 kN/m^2
NO_x gas partial press. = 10 kN/m^2
Case 1. Model predictions excluding heterogeneous equilibria and rate dependence on nitric acid concentration
Case 2. Model predictions excluding heterogeneous equilibria and including rate dependence on nitric acid concentration
Case 3. Model predictions including heterogeneous equilibria and rate dependence on HNO_3 concentration

Line No.	Case	HNO_3 Outlet Conc., wt. %
1	1	Any
2	2	15
3	2	30
4	2	45
5	3	15
6	3	30
7	3	45

contribute up to 20% to the overall rate of absorption when NO*/N* is 0.1 and at 30°C. The contribution was found to increase with an increase in temperature.

The effect of temperature on the extent of NO_x removal is shown in Figure 6. At low HNO_3 concentrations, NO_x removal is practically independent of temperature. However, at high HNO_3 concentrations an optimum temperature was observed. At low temperatures, NO oxidation and the formation of N_2O_4 are favored. However, the value of absorption parameter $H(kD)^{1/2}$ increases with an increase in temperature. The combined effect of the above two factors results in an optimum temperature. It may be emphasized that the relative importance of the above two factors depends upon HNO_3 concentration and column height.

The effect of air flow rate on the extent of NO_x removal is shown in Figure 7. It can be seen that NO_x absorption is maximum when the air flow rate is 4×10^{-4} kmol/s. An increase in the air flow rate increases the oxygen partial pressure, whereas it decreases the gas phase residence time for NO oxidation. These two opposite factors result in an optimum flow rate. Joshi et al. (1985) have discussed this subject in detail.

Experimental Work and Discussion

Measurement of specific rates of absorption

For the estimation of rates of absorption, it is desirable to know the values of diffusivity, rate constant, and orders with respect to different species. The measurement of these individual parameters is extremely difficult. Fortunately, the rates of absorption can be determined if we know the value of the combined parameter $H_x(kD)_x^{1/2}$ as described by Eqs. 29, 30, and 31.

Experiments for determining $H_x(kD)_x^{1/2}$ values for NO_2 and N_2O_4 in water and mixed solutions of nitric and sulfuric acids were conducted in a stirred cell of 95 mm ID. Temperature was maintained by using a constant-temperature bath. The experimental setup is shown in Figure 8.

A gas stream constituting 19–20% NO_x was obtained as a product gas from the pilot plant for producing oxalic acid. The gas stream was at 65°C and contained water vapor. The stream was passed through a condenser where the outlet tem-

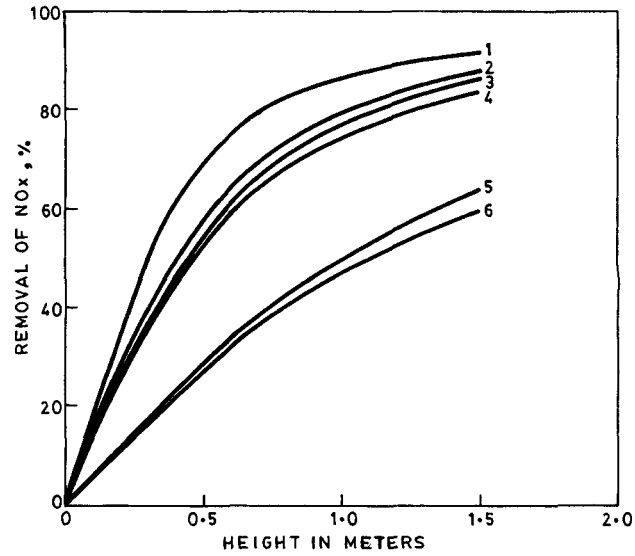

Figure 5. Effect of isothermal/adiabatic operation on extent of NO_x absorption.

Packed column dia. = 0.6 m
Packing = 38 mm Intalox saddles
Liquid superficial veloc. = 4 mm/s
Gas superficial veloc. = 0.1 m/s
$k_G a = 4.9 \times 10^{-4}$kmol/m^3·s·(kN/m^2)
$k_L a = 2.36 \times 10^{-3} \cdot s^{-1}$
$a = 154$ m^2/m^3
Liquid temp. = 323 K at 0 m ht.
Total press. = 709.0 kN/m^2
NO_x gas partial press. = 77 kN/m^2
NO*/N* = 0.5

Line No.	HNO_3 Conc., wt. %	Case
1	10	Isothermal
2	10	Adiabatic
3	30	Isothermal
4	30	Adiabatic
5	50	Isothermal
6	50	Adiabatic

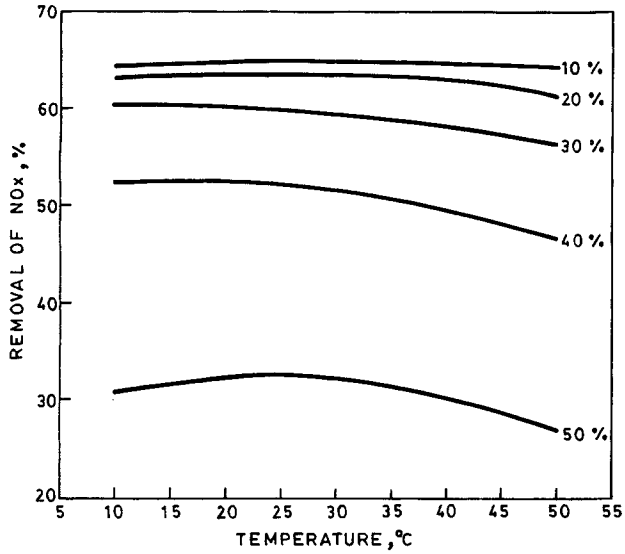

Figure 6. Effect of temperature and nitric acid concentration on extent of NO_x absorption.

Packed column dia. = 0.6 m, ht. = 0.5 m
Packing = 38 mm Intalox saddles
Liquid superficial veloc. = 6 mm/s
Gas superficial veloc. = 0.1 m/s
$k_G a = 1.25 \times 10^{-3}$ kmol/m^3·s·(kN/m^2) for NO
$k_L a = 1.5 \times 10^{-2}$·s^{-1}
$a = 125$ m^2/m^3
Total press. = 303.33 kN/m^2
NO_x gas partial press. = 33 kN/m^2
$NO^*/N^* = 0.05$
O_2 partial press. = 10% excess
H_2O partial press. = saturated

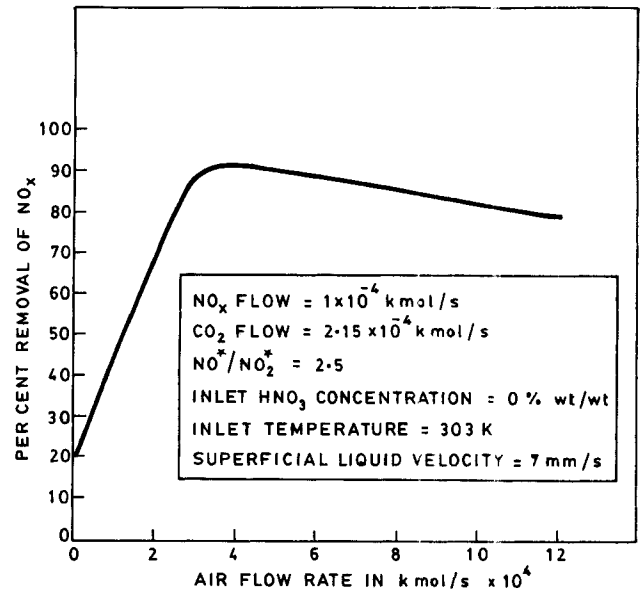

Figure 7. Effect of air flow rate on extent of NO_x absorption

perature was controlled to equal the desired temperature in the stirred cell. The gas stream leaving the condenser was saturated with water vapor. It was analyzed for divalent and tetravalent nitrogen oxides. Over 96% of NO_x was in the form of NO_2^*. The gas stream was introduced to the stirred cell through a rotameter. The flow rate was adjusted in such a way that the extent of absorption was less than 10%. This eliminated the uncertainty regarding gas phase backmixing because the extreme plug flow and backmixed behaviors will differ the rates of absorption by about 5%. We assumed completely backmixed behavior.

In all the experiments, the absorbent quantity was 120 mL and absorption was carried out for 300 s. During this period there was no appreciable change in the absorbent quantity because of either evaporation or condensation.

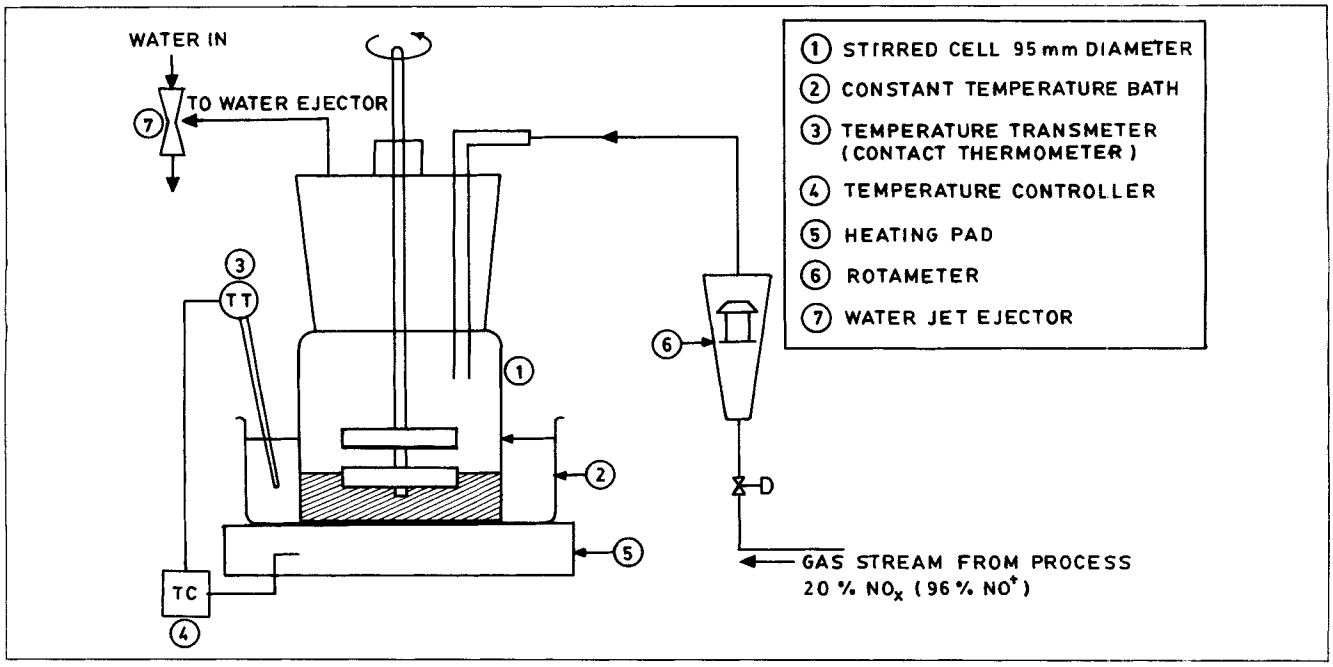

Figure 8. Experimental setup in stirred cell.

The effect of stirrer speed was investigated in the range of 0.167 to 1.33 r/s. The liquid surface was flat, without any vortex. It was observed that the specific rate of absorption was independent of the stirrer speed when the speed exceeded 0.67 r/s. This also indicates that there is no effect of gas- and liquid-side mass transfer coefficients (k_G and k_L) when the speed exceeds 0.67 r/s. It also indicates complete homogeneity of the liquid phase. Since the absorption operation was found to be independent of k_L, it means that absorption does not conform to the instantaneous reaction regime. All the above evidence indicates that the absorption operation falls in a fast pseudo mth-order reaction regime.

Water, 40% sulfuric acid, and mixed acid solutions containing nitric acid and 40% sulfuric acid were used as absorbents. A few experiments were also conducted to evaluate the effect of temperature on the values of the absorption parameter $H_x(kD)_x^{1/2}$.

Tetravalent nitrogen oxides (NO_2^*) constituted more than 96% of the NO_x gas used in the experiments. Under these conditions the partial pressure of divalent nitrogen oxides (p^i_{NO} and $p^i_{N_2O_3}$) was negligible. It was expected that the values of $[H^{3/2}(2/3\ kD)^{1/2}]_{NO_2}$ and $[H(kD)^{1/2}]_{N_2O_4}$ in H_2SO_4 would be lower than those in water due to the presence of electrolyte. It was assumed that

$$\frac{[H^{3/2}(2/3kD)^{1/2}]_{NO_2,\text{water}}}{[H^{3/2}(2/3kD)^{1/2}]_{NO_2,H_2SO_4}} = \frac{H(kD)^{1/2}]_{N_2O_4,\text{water}}}{[H(kD)^{1/2}]_{N_2O_4,H_2SO_4}} \quad (42)$$

The specific rate of formation of HNO_3 by the absorption of NO_x gas is given by the following equation:

$$R_{HNO_3} = 4/3R_{N_2O_4} + 2/3R_{NO_2}$$

$$= 4/3\ [H(kD)^{1/2}]_{N_2O_4,H_2SO_4}\ p^i_{N_2O_4}$$

$$+ 2/3\ [H^{3/2}(2/3kD)^{1/2}]_{NO_2,H_2SO_4}\ (p^i_{NO_2})^{3/2} \quad (43)$$

The interfacial partial pressures of NO_2 and N_2O_4 are related by Eq. 13. The following equation is obtained by substituting Eqs. 13 and 42 in Eq. 43:

$$R_{HNO_3} = 4/3\ [H(kD)^{1/2}]_{N_2O_4,H_2SO_4}(K_2(p^i_{NO_2})^2$$

$$+\frac{2}{3}\frac{[H^{3/2}\ (2/3kD)^{1/2}]_{NO_2,\text{water}}}{[H(kD)^{1/2}]_{N_2O_4,\text{water}}}(p^i_{NO})^{3/2}) \quad (44)$$

The value of $[H(kD)^{1/2}]_{N_2O_4,H_2SO_4}$ was obtained from Eq. 44 by using the experimental values of the specific rate of formation of HNO_3.

The value of $[H(kD)^{1/2}]_{N_2O_4}$ for water was found to be 7.6×10^{-6} kmol/m$^2\cdot$s$\cdot(kN/m^2)$ at 30°C. This value is in agreement with those reported in the literature (Sherwood et al., 1975; Joshi et al., 1985). The values of $H(kD)^{1/2}$ for N_2O_4 at various acid concentrations are given in Table 3. It can be seen that the value decreases with an increase in the concentration of nitric acid. Further, $[H(kD)^{1/2}]_{N_2O_4}$ was found to increase with an increase in temperature. It was thought desirable to develop a correlation for $[H(kD)^{1/2}]_{N_2O_4}$ in the range of temperature and concentration covered in this work. The following correlations were found to hold.

Table 3. Experimental Values of $[H(kD)^{1/2}]_{N_2O_4}$ for 40% Sulfuric Acid

% NO_x = 19 Temp. 30°C Sulfuric acid conc., 40 wt. %	
Nitric Acid wt.%	$[H(kD)^{1/2}]_{N_2O_4}$, [kmol/m$^3\cdot$s(kN/m^2)] $\times 10^6$
0.0	2.95
5.0	2.60
10.0	2.29
15.0	1.12
20.0	0.60
Nitric acid, 0.0 wt. % Sulfuric acid, 40 wt. %	
Temp. °C	$[H(kD)^{1/2}]_{N_2O_4}$, [kmol/m$^2\cdot$s(kN/m^2)] $\times 10^6$
40	3.3
20	2.8

$[H(kD)^{1/2}]_{N_2O_4}$, 30°C for water = 7.6×10^{-6} kmol/m$^2\cdot$s(kN/m^2)

For mixed acid solutions:

$$[H(kD)^{1/2}]_{N_2O_4} = 3.66\times10^{-5}e^{-6263.7/RT}(1 - 1.616\times10^{-2}W_N - 1.267\times10^{-3}W_N^2) \quad (45)$$

For water and nitric acid (Lefers and Van der Berg, 1982):

$$[H(kD)^{1/2}]_{N_2O_4} = 10^{[-3.215-1.424(W/(1-W)^{1.83}]}e^{-1,285.3/T} \quad (46)$$

$[H(kD)^{1/2}]_{N_2O_4}$ values in the presence of 40% sulfuric acid were found to be much lower than those found in water. This is because the activity of water decreases in the presence of sulfuric acid. The values of $[H(kD)^{1/2}]$ given by Eqs. 45 and 46 were used for the estimation of K_6 values for mixed acids. The equivalent nitric acid concentration was estimated on the basis of the same $[H(kD)^{1/2}]$ values. Table 4 gives the values for nitric acid concentration equivalent to mixed acid concentration. These values were used for determining K_6 from Eq. 25.

The values of $[H(kD)^{1/2}]_{N_2O_3}$ and $[H^{3/2}(2/3\ kD)^{1/2}]_{NO_2}$ were assumed to vary (with respect to concentration of acids and temperature) in an identical manner to that of $[H(kD)^{1/2}]_{N_2O_4}$.

Table 4. Nitric Acid Concentration Equivalent to Mixed Acid Concentration

Wt. % HNO_3 in 40% H_2SO_4	$[H(kD)^{1/2}]_{N_2O_4}$ at 30°C	Equiv. wt. % HNO_3 in Water
5	2.70×10^{-6}	36.36
10	2.168×10^{-6}	38.55
15	1.44×10^{-6}	41.93
20	0.519×10^{-6}	47.97

Table 5. Details of Experimental Setup

	Column 1	Column 2	Column 3
Diameter	0.254 m	0.254 m	0.8 m
Packed height	4.8 m	4.8 m	1.5 m
Total height	6.0 m	6.0 m	3.0 m
Packing type	Pall ring	Pall ring	Intalox saddle
Size	16 mm	16 mm	25 mm
Material	SS 316	SS 316	Ceramic
No. support plates	2	2	1
Liquid distributor	1	1	1
Plate heat exchanger	2.5 m^2	2.5 m^2	None
Pump			
Capacity, m^3/hr	3	3	9
Head, m water	18	18	22.5
Material	Polypro-pylene	Polypro-pylene	SS 316
Experimental Conditions			
V_L	5-6 mm/s	5-6 mm/s	5-6 mm/s
HNO_3 conc., wt. %	10.5	5.6	3
ρ_L, kg/m^3	1,350	1,350	1,350
V_G, m/s	0.2-0.3	0.2-0.25	0.2-0.25
% NO_x at inlet	20-23	8-12	3-6

Absorption of NO_x in a series of packed columns

Experiments were conducted in three continuous, countercurrently operated packed columns in series. Details pertaining to column dimensions and internals are given in Table 5. The first two columns were 0.254 m ID and 6 m tall. The third column was 0.8 m ID. and 3 m tall. The experimental setup is shown in Figure 9.

These three columns were used for the recovery of NO_x gases generated in the manufacture of oxalic acid. The process consists of oxidation of monosaccharides using mixed acid (40 wt. % sulfuric acid and 14-15 wt. % nitric acid). The oxidation reactions are as follows (Kirk and Othmer, 1981):

(a) $C_6H_{12}O_6 + 12HNO_3 \rightarrow 3C_2H_2O_4 \cdot 2H_2O + 3H_2O + 3NO + 9\ NO_2$

(b) $4C_6H_{12}O_6 + 18HNO_3 + 3H_2O \rightarrow 12C_2H_2O_4 \cdot 2H_2O + 9N_2O$

(c) $C_6H_{12}O_6 + 6HNO_3 \rightarrow 3C_2H_2O_4 \cdot 2H_2O + 6NO$

(d) $C_6H_{12}O_6 + 12HNO_3 \rightarrow 6CO_2 + 12H_2O + 6NO + 6NO_2$

These reactions were carried out in two stirred-tank reactors operated in series. The off-gases consist mainly of NO_x and carbon dioxide (some CO_2 is generated due to complete oxidation). The volumetric flow rate of this stream was measured using a precalibrated orifice meter. To this stream, a measured quantity of air was continuously added. The gaseous mixture was passed through a column that provided sufficient residence time (Joshi et al., 1985) for 95% conversion of divalent to tetravalent nitrogen oxides. The oxidized stream formed the gaseous feed for column 1. Some NO_x absorption occurred in column 1 and the remaining gases entered column 2 and subsequently column 3.

The liquid product from the reactors consisted of sulfuric acid (40 wt. %), product oxalic acid (11-12 wt. %), and unreacted nitric acid (0.5 wt. %). Oxalic acid was separated by cooling crystallization. The mother liquor was used for the recovery of NO_x gases and entered the liquid circulation loop of column 3. The average composition of the liquid phase for column 3 is given in Table 5. The overflow from the column 3 storage tank was added to the circulation loop of column 2, and overflow of the column 2 storage tank was added to the circulation loop of column 1. The overflow of column 1 was

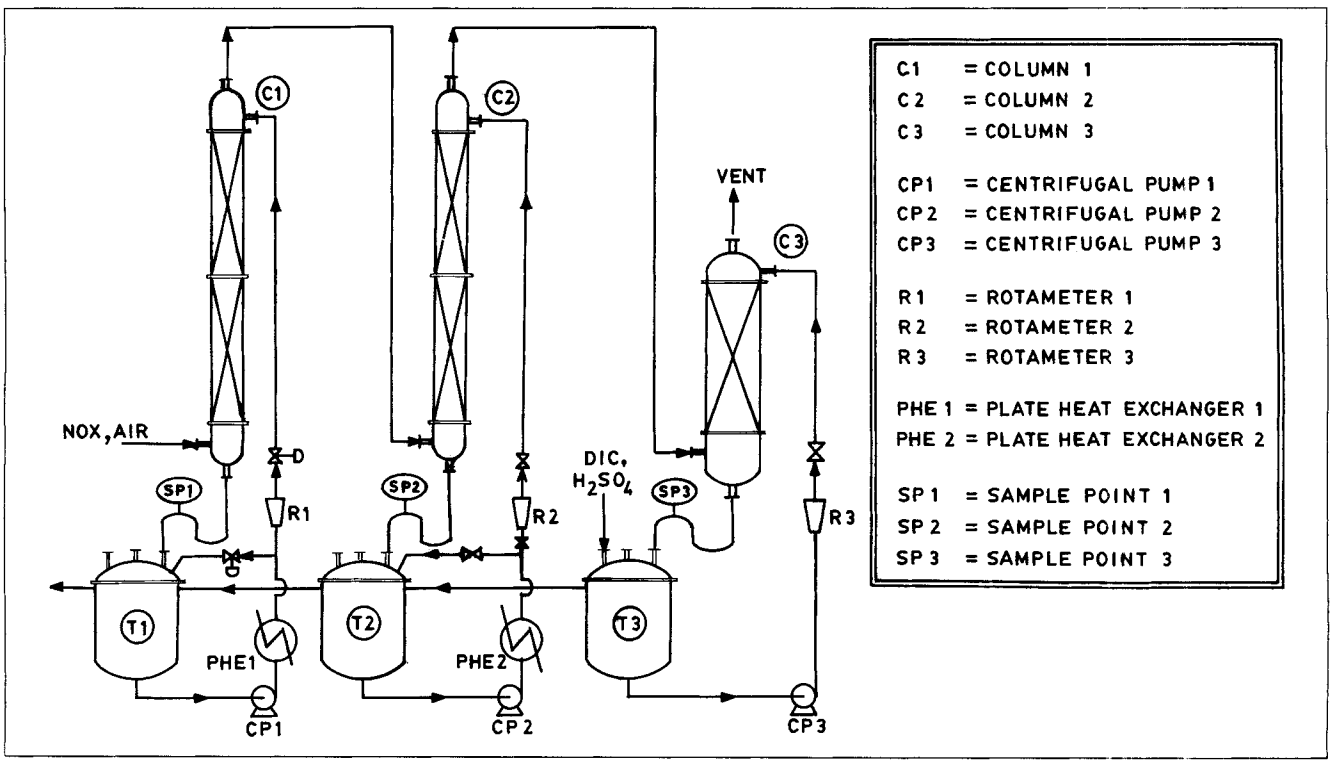

Figure 9. Three-column absorption system.

Table 6. Comparison between Model Predictions and Experimental Observations

Total gas flow = 7.1×10^{-4} kmol/s
NO_x flow = 1.78×10^{-4} kmol/s
NO*/N* = 0.72
Air flow = 4.17×10^{-4} kmol/s

	Column 1	Column 2	Column 3
Actual Removal of No_x, %			
Simulation	52.27	12.9	4.85
Experiment	59.5	12.3	4.9
Actual NO*/N* at Outlet			
Simulation	0.63	0.655	0.688
Experiment	0.565	0.629	0.70
Equilibrium Removal of NO_x, %			
Simulation	54.1	13.2	5.1
Average Conc. %			
Nitric acid	11.25	6.05	3.1
Sulfuric acid	40.25	41.0	41.5
Pressure	Atm.	Atm.	Atm.
Liquid Temp., °C			
At inlet	31	31	31
At outlet			
Simulation	37.3	31.7	32
Experiment	36.0	32.0	32

recycled to the reactors after adjusting acid concentration (by adding concentrated nitric and sulfuric acids). The liquid phase in all three columns was circulated to get a sufficiently good flow rate for wetting of the packings. In each recycle stream, the plate heat exchanger was incorporated to maintain the temperature within ±1°C.

The composition of the gas and the temperature were measured at the inlets and outlets of the columns. The liquid phase concentrations and flow rates were also measured. Liquid phase concentration was measured by fixing the acid mixture in an excess quantity of sodium hydroxide. The concentrations of sodium nitrate and sodium sulfate were measured using an ion chromatograph. Calibration charts were constructed by using standard samples of $NaNO_3$ and Na_2SO_4. The liquid phase

Table 7. Details of Experimental Setup

	Column 1	Column 2
Diameter	0.80 m	0.80 m
Packed height	6.0 m	6.0 m
Total height	7.0 m	10.0 m
Packing type	Intalox saddle	Intalox saddle
Size	37 mm	37 mm
Material	Ceramic	Ceramic
No. support plates	2	2
Liquid distributor	1	1
Plate heat exchanger	15.0 m^2	None
Pump		
Capacity, m^3/h	15	15
Head, m of water	25	25
Material	SS 316	SS 316
Experimental Conditions		
V_L	5-6 mm/s	5-6 mm/s
HNO_3 conc., wt. %	6.0	2.5
ρ_L, kg/m^3	1,350	1,350
V_G, m/s	0.14	0.14
% NO_x at inlet	14	7

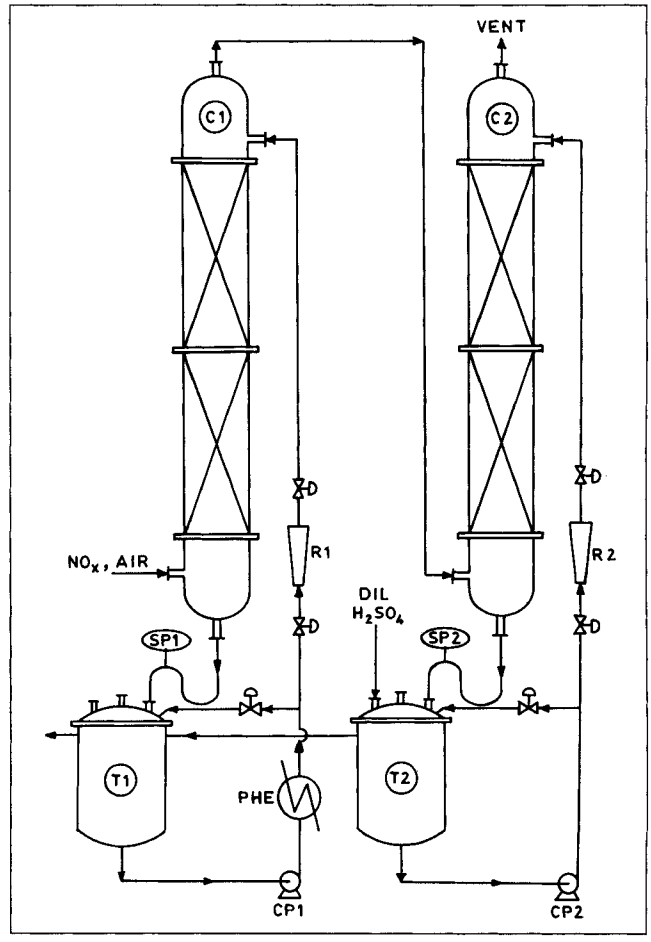

Figure 10. Two-column absorption system.

C1, C2, columns
CP1, CP2, centrifugal pumps
R1, R2, rotameters
PHE, plate heat exchanger
SP1, SP2, sample points

flow rate was measured by using a precalibrated rotameter. Details pertaining to the superficial gas velocity, superficial liquid velocity, temperature of operation, and the concentrations of various species are given Table 5. The percentage removal of NO_x in all the columns is summarized in Table 6. For the purpose of comparison, the results of model predictions are also given in Table 6. A favorable comparison (within 15% for column 1 and within 5% for columns 2 and 3) can be seen between the predicted and experimental values of conversion with respect to NO_x. The predicted temperature of the column 1 outlet is somewhat higher than the measured temperature. This was because the column was not insulated and the heat losses were not included in the model.

Experiments were also carried out in two 0.8 m ID packed columns operated in series. The flow sheet is given in Figure 10. The qualitative description of the process is the same as that for Figure 9. The details of the equipment are given in Table 7. A comparison between model predictions and experimental observations is given in Table 8. It can be seen that the agreement is within 5%. It may be emphasized that the inlet values of NO*/N* are markedly different for the first columns in Tables 6 and 8, and even then the agreement is good.

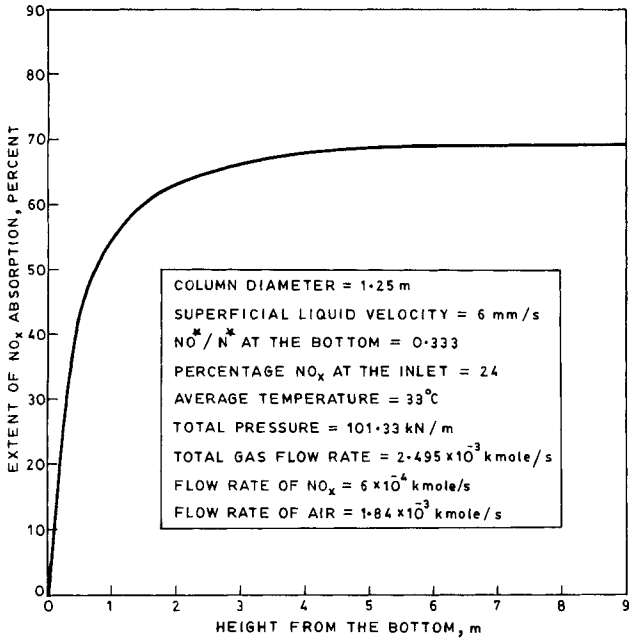

Figure 11. Effect of column height on the extent of NO_x absorption.

The extent of NO_x absorption increases with an increase in the packed height, Figure 11. It can be seen from Figure 11 that the rate of NO_x absorption is high in the bottom region. However, the rate becomes very low when the packed height exceeds about 4 m. At the bottom, the partial pressures of NO_2 and N_2O_4 are high compared with the equilibrium partial pressures for a given nitric acid concentration, Eqs. 23-28. Therefore, the rate of NO_x absorption, Eqs. 29-32, is high at the bottom. As the height increases, the driving force continuously decreases. Above a certain height—say 4 m in Figure 11—the overall absorption operation is controlled by the oxidation of NO in the gas phase. Therefore, for large packed heights, the extent of NO_x removal is controlled by heterogeneous equilibrium. Thus, Tables 6 and 8 show a comparison between predictions and experimental observations where heterogeneous equilibrium was practically established.

Table 8. Comparison between Model Predictions and Experimental Observations

Total gas flow = 2.5×10^{-3} kmol/s
NO_x flow = 3.5×10^{-4} kmol/s
$NO^*/N^* = 0.107$
Air flow = 1.74×10^{-3} kmol/s

	Column 1	Column 2	Total
Actual Removal of NO_x, %			
Simulation	55.9	21.9	77.8
Experiment	56.3	20.7	77.0
Actual NO^*/N^* at outlet			
Simulation	0.318	0.239	—
Experiment	0.331	0.226	—
Equilib. Removal of NO_x, %			
Simulation	58	23.3	81.3
Average conc., %			
Nitric acid	6.0	2.5	—
Sulfuric acid	42.0	43.0	—
Pressure	Atm.	Atm.	—
Liquid Temp., °C			
At Inlet	31	31	—
At outlet			
Simulation	37.3	31.7	—
Experiment	36.0	32.0	—

Table 9. Extent of NO_x Removal in 250 mm ID Column*

Total flow rate of gas phase	7.1×10^{-4} kmol/s
Flow rate of NO_x	1.78×10^{-4} kmol/s
NO^*/N^* ratio at bottom	0.72
Flow rate of air	4.17×10^{-4} kmol/s
Column details are given in Table 5	
Superficial liquid velocity	6 mm/s
Mixed acid concentration is given in Table 6	
Removal of NO_x at 1 m height, %	
Simulation	39.2
Experimental	41.7
Extent of removal at 4.8 m height is given in Table 6	

*Column 1, Table 5

In order to check the validity of the mass transfer rates, Eqs. 29-32, the extent of NO_x removal was measured in the 250 mm ID column (column 1 in Table 5). The gas and liquid samples were withdrawn at a distance of 1 m from the bottom and at the top of the column. The results are given in Table 9. In 1 m packed height, heterogeneous equilibrium conditions are not established and the rate of mass transfer is the controlling step. The agreement between the model predictions and experimental observations can be seen to be within 5%.

It may be noted that in all five packed columns studied in this work, most of the liquid phase was recycled, as shown in Figures 9 and 10. As a result, the HNO_2 concentration in the liquid phase attains a constant composition, as reported by Counce and Perona (1983). This was indeed found to be true in the present set of experiments. Therefore, the contributions of HNO_2 formation and decomposition to the extent of NO_x absorption were not considered in the present model.

Conclusions

A mathematical model has been developed in which four new features have been included. These are:

1. Variations in the rates of absorption of NO_2, N_2O_3, and N_2O_4 with respect to concentration of nitric acid
2. Heterogeneous equilibria between NO, N_2O_3, N_2O_4, and nitric acid concentration
3. Formation of nitric acid in the gas phase
4. Complete energy balance

The new model is capable of incorporating the effects of maximum permissible concentration of nitric acid on NO_x absorption.

Specific rates of absorption of N_2O_4 in water and mixed acid solutions of sulfuric and nitric acids were measured in a stirred cell with flat interface. The observed rates of absorption in water were found to agree with the published literature. In mixed acid solutions, the specific rates of absorption were found to decrease with an increase in the nitric acid concentration. The following correlation was found to hold in the range of 0-20 wt. % HNO_3 in 40 wt. % sulfuric acid, and at 18-19 kN/m^2 partial pressure of tetravalent nitrogen oxides:

$$[H(kD)^{1/2}]_{N_2O_4} = 3.66 \times 10^{-5} e^{-6263.7/RT}(1 - 1.616 \times 10^{-2} W_N - 1.267 \times 10^{-3} W_N^2)$$

Absorption of NO_x gases was carried out in 254 mm and 800 mm ID packed columns. A favorable agreement was observed between the model predictions and experimental observations.

Notation

a = interfacial area, m^2/m^3
a_p = dry area of packing per unit volume, m^2/m^3
$[A^*]$ = saturation concentration of gas phase reactant in liquid phase
c_p^o = average specific heat of liquid phase, kcal/kmol·K
dh = differential height of column
d_p = nominal size of packings, m
D_x = diffusivity of component x, m^2/s
D_G = diffusivity in gas phase, m^2/s
D_L = diffusivity in liquid phase, m^2/s
f = friction factor
F = packing factor
G = flow rate of inerts, kmol/s
G^* = mass flow rate of gas stream $kg/m^2 \cdot s$
h = height from bottom of packed bed, m
H = total height of packed column, m
$H(kD)^{1/2}$ = absorption factor for fast pseudofirst-order reaction, $kmol/m^2 \cdot (kN/m^2) \cdot s$
$H_x(kD)_x^{1/2}$ = absorption factor for fast pseudofirst-order reaction for component x, $kmol/m^2 \cdot (kN/m^2) \cdot s$
ΔH = standard heat of reaction, kcal/kmol
H_{el} = solubility in electrolyte, $kmol/m^3 \cdot (kN/m^2)$
H_{NO} = solubility of NO in water, $kmol/m^3 \cdot (kN/m^2)$
H_w = solubility in water, $kmol/m^3 \cdot (kN/m^2)$
k_G = physical gas-side mass transfer coefficient, $kmol/m^2 \cdot s \cdot (kN/m^2)$
K_H = heterogeneous equilibrium constant, Eqs. 35, 36
k_L = physical liquid-side mass transfer coefficient, m/s
k_n = forward reaction rate constant for reaction n
k_{-n} = backward reaction rate constant for reaction n
K_n = equilibrium constant for reaction n
K_6 = heterogeneous equilibrium constant, Eqs. 34, 36
l = characteristic length of packing, m
L = flow rate of liquid, kmol/s
L^* = mass velocity of liquid, $kg/m^2 \cdot s$
L_w = latent heat of vaporization of water, kcal/kmol
m^o = mass flow rate of liquid, kmol/s
m = coefficient, Eq. 61
n = exponent, Eq. 61
N^* = total moles NO_x
NO^* = total moles divalent nitrogen oxides
NO_2^* = total moles tetravalent nitrogen oxides
p_i = partial pressure of inert in bulk of gas
p_x = partial pressure of component x in bulk of gas
p_x^b = limiting partial pressure of component x at gas–liquid interface
p_x^i = partial pressure of component x at gas–liquid interface
p_x^o = partial pressure of component x in bulk of gas phase
P_m = power consumed per unit weight of gas holdup, m^2/s^3
P_T = total pressure of gas, kN/m^2
ΔP = pressure drop in packed column
Q_1 = heat changes due to formation of N_2O_3 in bulk gas, kcal/s
Q_2 = heat changes due to formation of N_2O_4 in bulk gas, kcal/s
Q_3 = heat changes due to formation of HNO_3 in bulk gas, kcal/s
Q_4 = heat changes due to formation of HNO_2 in bulk gas, kcal/s
Q_5 = heat changes due to oxidation of NO in bulk gas, kcal/s
Q_6 = heat changes due to water evaporation in bulk gas, kcal/s
Q_G = total heat changes in gas phase, kcal/s
Q_L = total heat changes in liquid phase, kcal/s
Q_T = total heat change, kcal/s
R = universal gas constant, $(m^3 \cdot kN/m^2)/(kmol \cdot K)$
$Ra_{x,L}$ = rate of absorption of component x, $kmol/(m^3 s)$
$Ra_{x,G}$ = rate of gas phase mass transfer of component x, $kmol/(m^3 s)$
Re_L = Reynolds number for liquid
s = exponent, Eq. 55
S = cross-sectional area of column, m^2
Sc_G = Schmidt number for gas
T = temperature, K
ΔT = temperature difference, K
V_L = superficial liquid velocity, m/s
V_G = superficial gas velocity, m/s
W = wt. frac. HNO_3 in aqueous nitric acid solution
W_N = wt. % HNO_3 in mixed acid
X_x = kmol x ions per kmol water
$(X)_e$ = component X at exit of differential volume
$(X)_f$ = component X formed in differential volume
$(X)_i$ = component X at inlet of differential volume
$(X)_o$ = component X oxidized in differential volume
$(X)_v$ = component X vaporized in differential volume
$X_{(g)}$ = component X in gas phase
$X_{(l)}$ = component X in aqueous phase
Y_T = total moles gas per mol inert
Y_x = mol gaseous component x per mol inert
$(Y_x)_e$ = Y_x at exit of differential height
$(Y_x)_i$ = Y_x at inlet of differential height
Y_N^* = kmol reactive nitrogen per kmol inerts
Y_{NO}^* = kmol divalent nitrogen per kmol inerts
$Y_{H_2O}^*$ = kmol water in form of oxyacids and free water in gas phase per kmol inerts
Z = coefficient, Eq. 55

Greek letters

α = coefficient, Eq. C3
β = exponent of superficial liquid velocity, Eq. C3
γ = exponent of nominal packing diameter, Eq. C3
η = coefficient, Eq. C9
ρ_L = density of liquid, kg/m^3
ρ_G = density of gas, kg/m^3
μ_G = viscosity of gas
μ_L = viscosity of liquid
μ_W = viscosity of water
ϵ = voidage
ϵ_G = fractional gas holdup
ϵ_L = fractional liquid holdup
ϵ_S = fractional solid holdup

Subscripts

a = absorption
e = exit condition
f = formation
$G, (g)$ = gas phase
i = inlet condition
$L, (l)$ = liquid phase
T = total
v = vapor
x = x in NO_x

Literature Cited

Andrew, S. P. S., and D. Hanson, "The Dynamics of Nitrous Gas Absorption," *Chem. Eng. Sci.*, **14**, 105 (1961).

Carberry, J., "Some Remarks on Chemical Equilibrium and Kinetics in the Nitrogen Dioxide–Water System," *Chem. Eng. Sci.*, **9**, 189 (1958).

Carleton, A. J., and F. H. Valentin, *Proc. 4th Eur. Symp. Chem. Reaction Eng.* (suppl. *Chem. Eng. Sci.*), Pergamon, Oxford, 361 (1968).

Carta, G., and R. L. Pigford, *Ind. Eng. Chem. Fundam.*, **22**, 329 (1983).

Counce, R. M., and J. J. Perona, "Gas-Liquid Interfacial Area of a Sieve Plate with Down Comers and 0.6% Perforations," *Ind. Eng. Chem. Proc. Des. Develop.*, **18**, 562 (1979a).
Counce, R. M., and J. J. Perona, "Gaseous Nitrogen Oxide Absorption in a Sieve Plate Column," *Ind. Eng. Chem. Fundam.*, **18**, 400 (1979b).
Counce, R. M., and J. J. Perona, "A Mathematical Model for Nitrogen Oxide Absorption in a Sieve Plate Column," *Ind. Eng. Chem. Proc. Des. Develop.*, **19**, 426 (1980).
Counce, R. M., and J. J. Perona, "Scrubbing of Gaseous Nitrogen Oxides in Packed Towers," *AIChE J.*, **29**, 26 (1983).
Danckwerts, P. V., *Gas-Liquid Reactions,* McGraw-Hill, New York (1970).
Emig, G., K. Wohlfahrt, and U. Hoffmann, "Absorption with Simultaneous Complex Reactions in Both Phases, Demonstrated by the Modeling and Calculation of Counter-Current Flow Columns for the Production of Nitric Acid," *Comput. Chem. Eng.*, **3**, 143 (1979).
Holma, H., and J. Sohlo, "A Mathematical Model for an Absorption Tower of Nitrogen Oxides in Nitric Acid Production," *Comput. Chem. Eng.*, **3**, 135 (1979).
Hoftizer, P. J., and F. J. G. Kwanten, "Absorption of Nitrous Gases," G. Honhabel, *Gas Purification Processes for Air Pollution Control,* Butterworths, London (1972).
Joshi, J. B., V. V. Mahajani, and V. A. Juvekar, "Absorption of NO_x Gases," *Chem. Eng. Commun.*, **33**, 1 (1985).
Kameoka, V., and R. L. Pigford, "Absorption of Nitrogen Dioxide into Water, Sulfuric Acid, Sodium Hydroxide, and Alkaline Sodium Sulfite Aqueous Solutions," *Ind. Eng. Chem. Fundam.*, **16**, 163 (1977).
Kirk and Othmer, *Encyclopedia of Chemical Technology,* 3rd ed., Wiley, New York, **16**, 623 (1981).
Koukolik, M., and J. Marek, *Proc. 4th Eur. Symp. Chem. React. Eng.* (suppl. *Chem. Eng. Sci.*), Pergamon, Oxford, 347 (1968).
Koval, E. J., and M. S. Peters, "Reaction of Aqueous Nitrogen Dioxide," *Ind. Eng. Chem.*, **52**, 1011 (1960).
Lefers, J. B., and P. J. Van der Berg, "Absorption of NO_2/N_2O_4 into Diluted and Concentrated Nitric Acid," *Chem. Eng. J.*, **23**, 211 (1982).
Mahajani, V. V., "Figuring Packed-Tower Diameter," *Chem. Eng.*, Sept. 20, 132 (1982).
Mahajani, V. V., and J. B. Joshi, "Mass Transfer in Packed Column: A Quick Look," (in preparation, 1990).
Makhotkin, A. F., and A. M. Shamsutdinov, *Khim. Khim. Tekhnol.*, **19**(9), 1411 (1976).
Matasa, C., and E. Tonca, *Basic Nitrogen Compounds,* Chemical Pub. Co., New York (1973).
Niranjan, K., V. G. Pangarkar, and J. B. Joshi, "Estimate Tower Pressure Drop," *Chem. Eng.*, June 27, 67 (1983).
Onda, K., E. Sada, T. Kobayashi, S. Kito, and K. Ito, "Salting Out Parameters of Gas Solubility in Aqueous Salt Solutions," *J. Chem. Eng. Japan,* **3**, 18 (1970).
Sada, E., H. Kumazawa, N. Hayakawa, I. Kudo, and T. Kondo, "Absorption of NO in Aqueous Solutions of $KMnO_4$," *Chem. Eng. Sci.*, **32**, 1171 (1977).
Sherwood, T. K., R. L. Pigford, and C. R. Wilke, *Mass Transfer,* McGraw-Hill, New York (1975).
Selby, G. W., and R. M. Counce, "Aqueous Scrubbing of Dilute Nitrogen Oxide Gas Mixtures," *Ind. Eng. Chem. Res.*, **27**, 1917 (1988).

Appendix A. Estimation of Partial Pressures of Various Gaseous Components on the Basis of Gas Phase Equilibria

The total number of moles in the gas per mole of inert is obtained by adding ratios of all gaseous species to mole of inert.

$$Y_T = Y_{NO} + Y_{NO_2} + Y_{N_2O_4} + Y_{N_2O_3} + Y_{HNO_3} + Y_{HNO_2} + Y_{H_2O} + Y_{O_2} + 1 \quad \text{(A1)}$$

where

$$Y_{N_2O_4} = K_2 (Y_{NO_2})^2 P_T / Y_T \quad \text{(A2)}$$

$$Y_{N_2O_3} = K_3 Y_{NO} Y_{NO_2} P_T / Y_T \quad \text{(A3)}$$

$$Y_{HNO_2} = (K_4 Y_{NO} Y_{NO_2} Y_{H_2O} P_T / Y_T)^{1/2} \quad \text{(A4)}$$

$$Y_{HNO_3} = \left[\frac{K_5 (Y_{NO_2})^3 Y_{H_2O}}{Y_{NO}} \frac{P_T}{Y_T} \right]^{1/2} \quad \text{(A5)}$$

In computing gas phase equilibria, we assume that there is no formation or removal of reactive nitrogen. Hence Y_N^*, total reactive nitrogen per mole of inert, is expressed as:

$$Y_N^* = Y_{NO} + Y_{NO_2} + 2(Y_{N_2O_4}) + 2(Y_{N_2O_3}) + Y_{HNO_3} + Y_{HNO_2} \quad \text{(A6)}$$

whereas the extent of oxidation at any moment is expressed in the form of Y_{NO}^*, moles of divalent nitrogen per mole of inert:

$$Y_{NO}^* = Y_{NO} + Y_{N_2O_3} + 0.5(Y_{HNO_2}) - 0.5(Y_{HNO_3}) \quad \text{(A7)}$$

$Y_{H_2O}^*$ is moles of water in the form of oxyacids and free water vapor per mole of inert. It is expressed as:

$$Y_{H_2O}^* = Y_{H_2O} + 0.5(Y_{HNO_3}) + 0.5(Y_{HNO_2}) \quad \text{(A8)}$$

Equations A2 to A5 express $Y_{N_2O_4}$, $Y_{N_2O_3}$, Y_{HNO_2}, and Y_{HNO_3} in terms of Y_{NO}, Y_{NO_2}, Y_{H_2O}, and Y_T. When these are substituted in Eqs. A1, A6, A7, and A8, four equations in Y_{NO}, Y_{NO_2}, Y_{H_2O}, and Y_T are obtained. They are:

$$Y_T^2 - Y_T(Y_{NO} + Y_{NO_2} + Y_{H_2O} + Y_{O_2} + 1) - Y_T^{1/2}\{[K_5 P_T (Y_{NO_2})^3 Y_{H_2O}/Y_{NO}]^{1/2} + (K_4 P_T Y_{NO} Y_{NO_2} Y_{H_2O})^{1/2}\} - [K_3 P_T Y_{NO_2} Y_{NO} + K_2 P_T (Y_{NO_2})^2] = 0 \quad \text{(A9)}$$

$$Y_T(Y_N^* - Y_{NO} - Y_{NO_2}) - Y_T^{1/2}\{(K_4 P_T Y_{NO} Y_{NO_2} Y_{H_2O})^{1/2} + [K_5 P_T (Y_{NO_2})^3 Y_{H_2O}/Y_{NO}]^{1/2}\} - 2P_T[K_2 (Y_{NO_2})^2 - K_3 Y_{NO} Y_{NO_2}] = 0 \quad \text{(A10)}$$

$$Y_T(Y_{NO}^* - Y_{NO}) - 1/2\ Y_T^{1/2}\{(K_4 P_T Y_{NO} Y_{NO_2} Y_{H_2O})^{1/2} - [K_5 P_T (Y_{NO_2})^3 Y_{H_2O}/Y_{NO}]^{1/2}\} - K_3 P_T Y_{NO} Y_{NO_2} = 0 \quad \text{(A11)}$$

$$Y_T(Y_{H_2O}^* - Y_{H_2O}) - 1/2\ Y_T^{1/2}\{(K_4 P_T Y_{NO} Y_{NO_2} Y_{H_2O})^{1/2} + [K_5 P_T (Y_{NO_2})^3 Y_{H_2O}/Y_{NO}]^{1/2} = 0 \quad \text{(A12)}$$

For known molar concentrations of inerts, oxygen, total NO_x, and NO* to (N*) ratio, equilibrium partial pressures of all the gaseous species in the bulk gas can be estimated by

solving Eqs. A9-A12 simultaneously for Y_T, Y_{NO}, Y_{NO_2}, and Y_{H_2O}. Compositions of HNO_3, HNO_2, N_2O_3, and N_2O_4 are obtained from equilibria relations, Eqs. A2-A5.

Appendix B. Simplification of Eqs. 6-15, 23, 26-35

The following two equations are obtained by substituting Eqs. 6-15, 23, and 26-35 into Eqs. 34 and 35:

$$A_1[p^i_{NO_2} - A_2(p^i_{NO})^{1/3}]^{3/2} + A_3(p^i_{NO_2})^2 - A_4(p^i_{NO})^{2/3}] + A_5[p^i_{NO}p^i_{NO_2} - A_2(p^i_{NO})^{4/3}] + A_7[(p^i_{NO})^{1/2}(p^i_{NO_2})^{1/2} - A_8(p^i_{NO})^{2/3}] + A_9(p^i_{NO})(p^i_{NO_2}) + A_{10}(p^i_{NO})^{1/2}(p^i_{NO_2})^{1/2} + A_{11}p^i_{NO} + A_{12} = 0 \quad \text{(B1)}$$

where

$$A_1 = \{\underline{a}\,(H_{NO_2})^{3/2}\,[(2/3\,kD)_{NO_2}]^{1/2}\}/3$$

$$A_2 = 1/K_2^{1/2}K_6^{1/3}$$

$$A_3 = \{2K_2\,\underline{a}\,H_{N_2O_4}\,[(kD)_{N_2O_4}]^{1/2}\}/3$$

$$A_4 = 1/(K_2\,K_6^{2/3})$$

$$A_5 = \{K_3\,\underline{a}\,H_{N_2O_3}\,[(Dk)_{N_2O_3}]^{1/2}\}/3$$

$$A_7 = (K_4\,p^i_{H_2O})^{1/2}\,K_L\underline{a}H_{HNO_2}/6$$

$$A_8 = 1/(K_2^{1/2}K_6^{1/3})^{1/2}$$

$$A_9 = -K_3\,(k_G\underline{a})_{N_2O_3}$$

$$A_{10} = -(K_4\,p^i_{H_2O})^{1/2}\,(k_G\underline{a})_{HNO_2}/2$$

$$A_{11} = -(k_G\underline{a})_{NO}$$

$$A_{12} = (k_G\underline{a})_{NO}p^o_{NO} + (k_G\underline{a})_{HNO_2}p^o_{HNO_2}/2 + (k_G\underline{a})_{N_2O_3}p^o_{N_2O_3}$$

and

$$B_1[p^i_{NO_2} - B_2(p^i_{NO})^{1/3}]^{3/2} + B_3p^i_{NO_2} + B_4[(p^i_{NO_2})^2 - B_5(p^i_{NO})^{2/3}] + B_6(p^i_{NO_2})^2 + B_7[p^i_{NO}p^i_{NO_2} - B_2(p^i_{NO})^{4/3}] + B_9[(p^i_{NO}p^i_{NO_2})^{1/2} - B_{12}(p^i_{NO})^{2/3}] + B_8(p^i_{NO})(p^i_{NO_2}) + B_{10}(p^i_{NO_2}p^i_{NO})^{1/2} + B_{11} = 0 \quad \text{(B2)}$$

where

$$B_1 = 3A_1$$

$$B_2 = A_2$$

$$B_3 = (k_G\underline{a})_{NO_2}$$

$$B_4 = 3A_3$$

$$B_5 = A_4$$

$$B_6 = 2K_2\,(k_G\underline{a})_{N_2O_4}$$

$$B_7 = 3A_5$$

$$B_8 = -A_9$$

$$B_9 = 3A_7$$

$$B_{10} = -A_{10}$$

$$B_{11} = -(k_G\underline{a})_{NO_2}p^o_{NO_2} - (k_G\underline{a})_{HNO_2}p^o_{HNO_2}/2 - (k_G\underline{a})_{N_2O_3}p^o_{N_2O_3} - 2(k_G\underline{a})_{N_2O_4}p^o_{N_2O_4}$$

$$B_{12} = A_8$$

Appendix C. Estimation of Design Parameters and Physical Properties

The column diameter was estimated on the basis of flooding calculations. The correlation (Mahajani, 1982) used to determine flooding conditions is:

$$\ln \overline{Y} = -3.3861 - 1.0814 \ln \overline{X} - 0.1273 (\ln \overline{X})^2 \quad \text{(C1)}$$

where

$$\overline{Y} = \frac{(G^*)^2 F\,\mu_L^{0.1}}{\rho_L\,\rho_G}$$

$$\overline{X} = \frac{L^*}{G^*}\left\{\frac{\rho_G}{\rho_L}\right\}^{1/2}$$

Packing factor F was calculated from the equation,

$$F = Z(d_p)^{-s} \quad \text{(C2)}$$

The correlation employed for computing the effective interfacial area (Joshi et al., 1985) in packed column is

$$\underline{a} = \frac{\alpha\,V_L\beta(d_p)\gamma}{\epsilon^3} \quad \text{(C3)}$$

Values for α, β, and γ for different packings are as in Table A1. Mahajani and Joshi (1990) have developed correlations for gas-side and liquid-side mass transfer coefficients based on turbulence intensity. They have shown that the following correlation for the gas-side mass transfer coefficient holds for all the packings.

$$\frac{(k_GRT)l}{D_G} = 0.553\left[\frac{(P_m l)^{1/3}\,l\,\rho_G}{\mu_G}\right]^{0.62}(Sc_G)^{1/3}\left(\frac{p_x}{p_i}\right) \quad \text{(C4)}$$

where P_m is the power consumption per unit mass of the gas

$$P_m = \frac{fa_pV_G^3}{[6(\epsilon - \epsilon_L)^4]} \quad \text{(C5)}$$

l is the characteristic length of packing; its value depends on type of packing, Table A1.

Liquid holdup in the packed column is computed as

$$\epsilon_L = \left[1.53\times10^{-4} + 2.9\times10^{-5}Re_L^{0.66}\left(\frac{\mu_L}{\mu_W}\right)^{0.75}\right]d_p^{-1.2} \quad \text{(C6)}$$

Table A1. Values of Constants in Eqs. C1-C11

Packings	f	m	$n=\gamma$	l	α	β	Z	s	$\eta\times10^{-2}$
Raschig rings	3.76	4.53	−1.015	$0.5d_p$	8.0	0.403	27,800	1.533	2.1
Pall rings	2.17	3.96	−1.07	$0.1d_p$	28.4	0.5	843	0.913	4.4
Intalox saddles	2.03	6.74	−1.0	$0.25d_p$	19.6	0.478	7,091	1.337	2.7

where the Reynolds number is given by

$$Re_L=\frac{d_p V_L \rho_L}{\mu_L \epsilon} \tag{C7}$$

The specific surface area is calculated from the packing diameter as

$$a_p=m(d_p)^n \tag{C8}$$

Values of m and n for different packings are given in Table A1.

Liquid-side mass transfer coefficient k_L has been estimated from the following correlation:

$$(k_L l/D_L)=\eta Re_L\left(\frac{\mu_L}{\rho_L D_L}\right)^{0.5} \tag{C9}$$

Values of coefficient η are listed in Table A1.

Pressure drop in the packed column was estimated by the following correlation (Niranjan et al., 1983)

$$(\Delta P/h)=\frac{f(G^*)^2 a_p}{[6\ \rho_G(\epsilon-\epsilon_L)]} \tag{C10}$$

Diffusivities of gases vary with temperature and pressure. For this purpose, the following correction was used.

$$D_x=D_{x,25^\circ C}(T/298.2)^{1.75}(101.33/P_T) \tag{C11}$$

The solubility of HNO_3 and HNO_2 in water is 2,090 and 0.484 kmol/m$^3\cdot$(kN/m^2), respectively (Joshi et al., 1985). The solubility of NO in water is given by the following equation:

$$\log_{10}(101.33\times H_{NO})=-1{,}463.32/T+2.178 \tag{C12}$$

The solubility of NO and HNO_2 in the presence of electrolytes like H_2SO_4 and HNO_3 was estimated by using the following equation:

$$\log_{10}(H_{el}/H_w)=-\Sigma K_s I \tag{C13}$$

where

H_w = solubility in water, kmol/m$^3\cdot$(kN/m^2)
H_{el} = solubility in electrolyte solution, kmol/m$^3\cdot$(kN/m^2)
K_s = salting-out parameter $= i^+ + i^- + i_g$

i^+ and i^- are contributions of cations and anions of the electrolyte, respectively, to the salting-out parameter and i_g is the contribution of the solute gas. Danckwerts (1970) and Onda et al. (1970) have reported the values of salting-out parameters for various cations, anions, and gases. The value of i_g for NO gas was reported by Sada et al. (1977). The value of i_g for HNO_3 was estimated from the vapor pressure of HNO_3 over nitric acid. The value of i_g for HNO_2 was assumed to be the same as that of HNO_3.

Appendix D. Heat Changes

Gas phase heat changes

Contribution to the heat changes from the gas phase are due to the following steps.

1. The rate of formation of N_2O_3 from NO and NO_2 in the differential element is given by:

$$(N_2O_3)_f=(N_2O_3)_e-(N_2O_3)_i+(N_2O_3)_a \tag{D1}$$

$$(N_2O_3)_f=G(Y_{N_2O_3,e}-Y_{N_2O_3,i})+Ra_{N_2O_3,l}Sdh \tag{D2}$$

The rate of heat generation due to N_2O_3 formation is:

$$Q_1=(N_2O_3)_f\,\Delta H_4 \tag{D3}$$

2. The rate of formation of N_2O_4 from NO_2 in the differential element is given by:

$$(N_2O_4)_f=(N_2O_4)h-(N_2O_4)_i+(N_2O_4)_a \tag{D4}$$

$$(N_2O_4)_f=G(Y_{N_2O_4,e}-Y_{N_2O_4,i})+Ra_{N_2O_4,l}Sdh \tag{D5}$$

The rate of heat generation due to N_2O_4 formation is:

$$Q_2=(N_2O_4)_f\,\Delta H_3 \tag{D6}$$

3. The rate of formation of HNO_3 in the differential element is given by:

$$(HNO_3)_f=(HNO_3)_e-(HNO_3)_i+(HNO_3)_a \tag{D7}$$

$$(HNO_3)_f=G(Y_{HNO_3,e}-Y_{HNO_3,i})+Ra_{HNO_3,G}Sdh \tag{D8}$$

The rate of heat liberated due to HNO_3 formation is:

$$Q_3=(HNO_3)_f\,\Delta H_6 \tag{D9}$$

4. The rate of formation of HNO_2 in the differential element is given by:

$$(HNO_2)_f=(HNO_2)_e-(HNO_2)_i+(HNO_2)_a \tag{D10}$$

$$(HNO_2)_f = G(Y_{HNO_2,e} - Y_{HNO_2,i}) + Ra_{HNO_2,L} Sdh \quad \text{(D11)}$$

The rate of heat liberated due to HNO_2 formation is:

$$Q_4 = (HNO_2)_f \, \Delta H_7 \quad \text{(D12)}$$

5. The rate of heat liberated due to the oxidation of NO is estimated from the knowledge of the rate of NO oxidation. It may be noted that NO is used in the N_2O_3 and HNO_2 formation and it is liberated during HNO_3 formation.

The mass balance for NO across the differential element is given by:

$$NO_{,o} = (NO_{,i} - NO_{,e}) - N_2O_{3,f} - 1/2 \; HNO_{2,f} + 1/2 \; HNO_{3,f} \quad \text{(D13)}$$

$$= G(Y_{NO,i} - Y_{NO,e} - Y_{N_2O_3,e} + Y_{N_2O_3,i} - 1/2 \; Y_{HNO_2,e} + 1/2 \; Y_{HNO_2,i} + 1/2 \; Y_{HNO_3,e} - 1/2 \; Y_{HNO_3,i}) - (Ra_{N_2O_3,L} + 1/2 \; Ra_{HNO_2,L} - 1/2 \; Ra_{HNO_3,G}) \; S \; dh) \quad \text{(D14)}$$

The rate of heat generation due to NO oxidation is given by:

$$Q_5 = (NO)_o \, \Delta H_1 \quad \text{(D15)}$$

Heat changes due to water evaporation

The rate of water evaporation in the differential element was obtained by material balance:

$$(H_2O)_v = (H_2O_{,e} - H_2O_{,i}) + 1/2 \; HNO_{3,f} + 1/2 \; HNO_{2,f} \quad \text{(D16)}$$

$$(H_2O)_v = G \; (Y_{H_2O,e} - Y_{H_2O,i} + 1/2 \; Y_{HNO_3,e} - 1/2 \; Y_{HNO_3,i} + 1/2 \; Y_{HNO_2,e} - 1/2 \; Y_{HNO_2,i}) + (1/2 \; Ra_{HNO_3,G} + 1/2 \; Ra_{HNO_2,L}) S \; dh \quad \text{(D17)}$$

$$Q_6 = (H_2O)_v \, L_w \quad \text{(D18)}$$

The total heat change in the gas phase is given by:

$$Q_G = Q_1 + Q_2 + Q_3 + Q_4 + Q_5 + Q_6 \quad \text{(D19)}$$

Heat changes due to absorption with chemical reaction

In the absence of information on heats of dissolution of gases the information on heats of formation of reactants and products was used to compute the heats of reactions.

Reactions under consideration for the heat balance are:

$$\text{(1)} \; 2 \; NO_{2(g)} + H_2O_{(l)} \rightarrow HNO_{3(l)} + HNO_{2(l)} \quad \text{(D20)}$$

$$\text{(2)} \; N_2O_{4(g)} + H_2O_{(l)} \rightarrow HNO_{3(l)} + HNO_{2(l)} \quad \text{(D21)}$$

$$\text{(3)} \; N_2O_{3(g)} + H_2O_{(l)} \rightarrow 2 \; HNO_{2(l)} \quad \text{(D22)}$$

$$\text{(4)} \; 3 \; HNO_{2(l)} \rightarrow HNO_{3(l)} + 2 \; NO_{(g)} + H_2O_{(l)} \quad \text{(D23)}$$

$$\text{(5)} \; HNO_{3(g)} \rightarrow HNO_{3(l)} \quad \text{(D24)}$$

$$\text{(6)} \; HNO_{2(g)} \rightarrow HNO_{2(l)} \quad \text{(D25)}$$

Heats of reaction are summarized in Table 2.

Heat liberated due to absorption with chemical reaction in the liquid phase is expressed as:

$$Q_L = (Ra_{NO_2,L}\Delta H_8 + Ra_{N_2O_4,L}\Delta H_9 + Ra_{N_2O_3,L}\Delta H_{10} + Ra_{HNO_3,G}\Delta H_{11} + Ra_{HNO_2,L}\Delta H_{12} + Ra_{NO,L}\Delta H_{13}) \; S \; dh \quad \text{(D26)}$$

Total heat change in the differential volume is the summation of all the heat changes.

$$Q_T = Q_G + Q_L \quad \text{(D27)}$$

Manuscript received June 12, 1990, and revision received Nov. 27, 1990.